for allyltri-*n*-butylstannane and tri-*n*-butyltin chloride (and lower sensitivity—0.1% natural abundance vs 8.7% for ^{119}Sn), the chemical shift for the allylic carbon of allyltri-*n*-butylstannane is highly diagnostic (9.2 ppm). Again, this signal was observed to persist for more than 1 h at −90 °C upon reaction of $(5)_2{\cdot}SnCl_4$ with allyltri-*n*-butylstannane, in marked contrast to the claims of Denmark and co-workers.

In summary, we find no evidence that transmetalation pathways intervene in the reactions of coordinatively saturated $SnCl_4$–aldehyde complexes with allyltri-*n*-butylstannane at low temperature, be they chelates or 2:1 complexes. We believe that our experiments demonstrate quite convincingly that transmetalation is only important under conditions where free $SnCl_4$ is present or where fast ligand exchange opens up vacant coordination sites on the metal, conditions that are identifiable via variable-temperature ^{119}Sn NMR spectroscopy of the complexes in the absence of allylstannane. The potential presence of free $SnCl_4$ cannot be addressed in the Denmark experiments which utilize ^{13}C observation. Although the reasons for the discrepancy between our results and those obtained by Denmark are not clear, we believe that differences in internal temperature are most probably responsible.

Acknowledgment. Financial support of this research by the National Institutes of Health through Grant GM-28961 is gratefully acknowledged. We also acknowledge the exchange of information between the Denmark group and our own on various occasions regarding the discrepancies between our results.

The Chemistry of Rhenium and Tungsten Porphyrin Complexes in Low Oxidation States. Synthesis and Characterization of Rhenium and Tungsten Porphyrin Dimers Containing Metal–Metal Multiple Bonds

James P. Collman,* James M. Garner, and L. Keith Woo

Contribution from the Department of Chemistry, Stanford University, Stanford, California 94305. *Received November 21, 1988*

Abstract: The coordination chemistry of rhenium and tungsten porphyrin complexes in low oxidation states is presented. $W^{IV}(Por)(Cl)_2$, $W^{II}(Por)(H_5C_6C{\equiv}CC_6H_5)$, and $W^{II}(OEP)(PEt_3)_2$ complexes [Por = 5,10,15,20-tetra(4-tolyl)porphyrin (TTP) or 2,3,7,8,12,13,17,18-octaethylporphyrin (OEP) dianions] were found to be similar to the analogous molybdenum porphyrin complexes by spectroscopic and magnetic measurements. The tungsten acetylene and phosphine complexes are suitable precursors to the diamagnetic, quadruply bonded $[W^{II}(OEP)]_2$ complex via the solid-state vacuum pyrolysis reaction previously developed for the $[Ru^{II}(Por)]_2$, $[Os^{II}(Por)]_2$, and $[Mo^{II}(Por)]_2$ complexes. The triply bonded $[Re^{II}(Por)]_2$ compounds were prepared by a similar pyrolysis reaction of the $Re^{II}(Por)(PEt_3)_2$ complexes. Population of a paramagnetic excited state for $[Re^{II}(OEP)]_2$ is postulated from solution ^1H NMR data but solid-state magnetic measurements indicate this dimer is diamagnetic. $[Re^{II}(OEP)]_2$ can be oxidized to yield mono- and dicationic dimeric complexes. UV–visible and vibrational spectroscopies indicate that these oxidations occur at the metal–metal bond rather than the porphyrin ligand.

Dimeric metalloporphyrin complexes joined by a metal–metal multiple bond represent a new class of binuclear metal complexes with M_2L_8 structures. As detailed earlier,[1] the porphyrin ligand allows opportunities and advantages to investigate the detailed nature of these bonds in ways that are unavailable with other classical inorganic ligands. Examples include the use of the porphyrin ligand to investigate the paramagnetism of the neutral ruthenium and osmium dimers by ^1H NMR,[2] as well as the use of meso-substituted porphyrins to obtain unique solution evidence for the existence of a δ bond in the molybdenum dimer.[3]

Our goal in this research has been to prepare an entire family of such compounds with all the formal metal–metal bond orders represented by substituting different divalent metal ions within the porphyrin macrocycle. Other classes of compounds that rival the dimetalloporphyrin family in terms of different metals, valence d electron counts, and bond orders are often supported with bridging bidentate ligands. An example of such a family is the dimetal tetracarboxylates. However, bridging ligands strongly influence the metal–metal bonding interaction, and systematic trends due solely to the metal–metal bonding are often masked by the ligand. The porphyrin ligand is more innocent in the metal–metal interaction by virtue of its nonbridging, rigid, square-planar geometry.[4] Hence, systematic trends of the structural, spectroscopic, and chemical properties within this family of compounds will likely be more salient, leading to new insights and questions concerning the nature of multiple bonds between metal atoms. Presently, the molybdenum,[1] ruthenium,[2] osmium,[1] rhodium,[5] and iridium[6] porphyrin dimers have been prepared; however, none of the divalent, four-coordinate, 3d metalloporphyrins show any tendency to form metal–metal bonded complexes. Therefore, completion of this family of compounds required the synthesis of the analogous rhenium and tungsten complexes.

Although rhenium and tungsten porphyrin complexes were first prepared 15 years ago, almost no low-valent complexes are described in the literature.[7] Herein, we report the coordination

(1) Collman, J. P.; Barnes, C. E.; Woo, L. K. *Proc. Natl. Acad. Sci. U.S.A.* **1983**, *80*, 7684.
(2) Collman, J. P.; Barnes, C. E.; Sweptson, P. N.; Ibers, J. A. *J. Am. Chem. Soc.* **1984**, *106*, 3500.
(3) Collman, J. P.; Woo, L. K. *Proc. Natl. Acad. Sci. U.S.A.* **1984**, *81*, 2592.
(4) Obviously, the macrocyclic ligand is not totally innocent in the metal–metal bonding interaction. Nonbonding repulsive forces between the two porphyrin moieties may indeed weaken the metal–metal bond to some degree.
(5) (a) Ogoshi, H.; Setsune, J.; Yoshida, Z. *J. Am. Chem. Soc.* **1977**, *99*, 3869. (b) Wayland, B. B.; Newman, A. R. *Inorg. Chem.* **1981**, *20*, 3093.
(6) Del Rossi, K. J.; Wayland, B. B. *J. Chem. Soc., Chem. Commun.* **1986**, 1653.

0002-7863/89/1511-8141$01.50/0

chemistry of rhenium and tungsten porphyrin complexes in low oxidation states and the synthesis and characterization of the corresponding metalloporphyrin dimers.

Experimental Section

Solvents and Reagents. All solvents for glovebox use were distilled from their blue or purple sodium benzophenone ketyl solutions (toluene, benzene, THF, and hexanes), from P_2O_5 (CH_3CN and CH_2Cl_2), or from $NaOCH_3$ (CH_3OH) under a dry nitrogen atmosphere. These dried solvents were subsequently degassed in the glovebox by bubbling box atmosphere gas through the solutions for 20–30 min. Deuterated solvents (CD_2Cl_2, $CDCl_3$, $C_6D_5CD_3$, and C_6D_6) were dried similarly and then degassed on a vacuum line (10^{-5} Torr) with three successive freeze–pump–thaw cycles. Triethylphosphine was dried by stirring over Al(Hg) for 24 h prior to use. DMF was stirred over $MgSO_4$ (24 h), filtered, vacuum distilled (76 °C, 39 Torr), and stored over activated (200 °C, 10^{-2} Torr) sieves (Linde, 4X). Argon for Schlenkware reactions was dried by passage over activated sieves. Flash chromatographic silica (EM Science, Kieselgel 60H), gravity alumina (Fischer, Neutral, 80–200 mesh), and Celite for glovebox use were predried at 300 °C overnight and then further dried and degassed under vacuum (300 °C, 10^{-2} Torr) for 24 h and stored in the glovebox. Alumina TLC plates were heated under vacuum (200 °C, 10^{-2} Torr) for 20 h and also stored in the glovebox. The following reagents were purchased commercially and used without further purification: $AgBF_4$, Si_2Cl_6, diphenylacetylene, proton sponge, and H_2OEP (Aldrich); $LiAlH_4$ (Alfa); anhydrous HCl (Linde); $W(CO)_6$ (Pressure Chemical). $[(Cp)_2Fe](BF_4)$,[8] $[W(CO)_4(Cl)_2]_2$,[9] $Re(OEP)(PEt_3)_2$, and $Re(TTP)(PEt_3)_2$,[10] H_2TTP,[11] $W(OEP)(O)(Cl)$,[12] and Al(Hg)[13] were prepared by literature procedures.

Instruments and Measurements. All manipulations of air-sensitive compounds were performed either in a glovebox, in Schlenkware, or on a vacuum line. The glovebox was a Vacuum/Atmospheres HE-553-2 Dri-Lab with a MO-40-1H Dri-Train under nitrogen atmosphere ($O_2 \leq$ 1 ppm). Oxygen levels were monitored with a AO 316-C trace oxygen analyzer. ^1H NMR spectra were recorded with a 300-MHz Nicolet NMC-300 instrument with a FT 1280 disk data system, and all chemical shifts are reported relative to tetramethylsilane. A Cary 219 spectrophotometer was used to record UV–visible spectra (300–825 nm). FAB mass spectroscopy was performed at the University of California—Berkeley chemistry department mass spectroscopy facility using an air-sensitive technique. The liquid matrix was sulfolane, and the calculated isotope intensities matched well with the observed molecular or fragment ion isotope clusters. Solution magnetic susceptibility measurements (21 °C) utilized the Evans method[14a] with Wilmad precision coaxial NMR tubes and are corrected for ligand diamagnetism with literature values.[14b,c]

W^V(TTP)(O)(Cl) (1). A suspension of H_2TTP (1.000 g, 1.49 mmol) and $W(CO)_6$ (0.900 g, 2.56 mmol) in DMF (20 mL) containing octane (2 mL) was degassed with nitrogen for 30 min and then refluxed for 24 h. Every 6 h, another aliquot of $W(CO)_6$ (0.900 g) was added to the cooled solution under nitrogen, and then the solution was reheated to reflux. The brown solution was cooled and poured into a brine solution. The precipitate was collected on a Celite pad and washed with water (75 mL). The pad was then washed with CH_2Cl_2 until the filtrate was colorless. The green–brown filtrate was concentrated and flash chromatographed (SiO_2, 4 × 12 cm, CH_2Cl_2). A brown impurity eluted with CH_2Cl_2 and was discarded. A 5% methanolic CH_2Cl_2 solution eluted the major green band. This band was evaporated, redissolved in CH_2Cl_2, and then treated with aqueous HCl (40 mL, pH 2) under nitrogen atmosphere[15] for 30 min with rapid stirring. The CH_2Cl_2 solution was separated from the aqueous phase and concentrated (5 mL). Hexanes (30 mL) were layered over the solution, and green needles crystallized upon cooling (–20 °C). These crystals were collected by filtration, washed with hexanes, and dried under vacuum (10^{-2} Torr, 50 °C) overnight (1.011 g, 75%). ^1H NMR ($CDCl_3$, ppm): H_β, 8.35 (very br s); aryl, 7.90 (br s); aryl, 7.64 (br s); CH_3, 2.69 (s). EIMS, *m/e*: 904, cluster, M^+; 869, cluster, $M^+ - Cl$. UV–vis (CH_2Cl_2) λ_{max}, nm (log ϵ): 340 (4.54), 468 (5.35), 602 (4.02), 648 (4.10). Anal. Calcd for $C_{48}H_{36}N_4OClW$: C, 63.76; H, 4.02; N, 6.20. Found: C, 63.55; H, 4.30; N, 5.99.

W^{IV}(OEP)$(Cl)_2$ (2). In the glovebox, a green solution of W(OEP)(O)(Cl) (500 mg, 0.651 mmol) in CH_2Cl_2 (10 mL) was prepared in a Schlenk tube (2 × 15 cm). The solution was treated with Si_2Cl_6 (0.2 mL, 1.2 mmol) and stirred for 4 h. The solution color became brown. The tube was sealed and taken out of the glovebox, and gaseous HCl diluted with argon was bubbled through the solution for 5 min. The solvent was evaporated to yield an air-sensitive, brown–blue solid. FABMS, *m/e*: 752, cluster, $M^+ - Cl$. μ_{eff} ($CDCl_3$) = 1.7 ± 0.2 μ_B.

W^{IV}(TTP)$(Cl)_2$ (3). This complex was prepared exactly as described for **2**. FABMS, *m/e*: 888, cluster, $M^+ - Cl$. μ_{eff} ($CDCl_3$) = 1.8 ± 0.2 μ_B.

W^{II}(OEP)$(H_5C_6C{\equiv}CC_6H_5)$ (4). In the glovebox, $LiAlH_4$ (200 mg, 5.3 mmol) and diphenylacetylene (800 mg, 4.5 mmol) in toluene (4.5 mL) containing THF (0.3 mL) was stirred for 30 min. **2** (500 mg, 0.635 mmol) was added to this suspension as a solid over a 15-min period. A gas evolved with each addition, and the solution color became purple–red. The mixture was stirred for 1 h, and then the solvent was evaporated. The residue was dissolved in toluene, filtered through a Celite pad, and then evaporated again in a Schlenk tube. The excess diphenylacetylene was distilled (80 °C, 10^{-2} Torr) from this residue overnight, and the porphyrinic product was flash chromatographed (SiO_2, 1 × 5 cm, toluene) in the glovebox. The eluate was evaporated and dried under vacuum to yield a purple solid (240 mg, 43%). ^1H NMR (C_6D_6, ppm): H_{meso}, 9.42 (s, 4 H); CH_2CH_3, 3.75 (q, J = 7.6 Hz, 16 H); CH_2CH_3, 1.71 (t, J = 7.5 Hz, 24 H). ^3H NMR (C_6D_6, ppm), acetylene: H_m, 6.57 (t, J = 7.5 Hz, 4 H); H_p, 6.30 (t, J = 7.3 Hz, 2 H); H_o, 4.99 (d, J = 8.6 Hz, 4 H). FABMS, *m/e*: 1030, cluster, M^+. UV–vis (toluene) λ_{max}, nm (log ϵ): 307 (4.31), 402 (5.06), 530 (4.00), 563 (4.21), 572 (4.23), 616 sh (3.53), 792 (3.12). Anal. Calcd for $C_{50}H_{54}N_4W$: C, 67.11; H, 6.08; N, 6.26. Found: C, 67.16; H, 5.95; N, 6.40.

W^{II}(TTP)$(H_5C_6C{\equiv}CC_6H_5)$ (5). This complex was prepared by the procedure described for **4** starting with **3** (100 mg). Yield: 58 mg, 52%. ^1H NMR (C_6D_6, ppm): H_β, 6.72 (s, 8 H); H_o, 7.22 (d, J = 7.7 Hz, 8 H); H_m, 7.54 (d, J = 7.8 Hz, 8 H); CH_3, 2.33 (s, 12 H). ^1H NMR (C_6D_6, ppm), acetylene: H_m, 7.03 (t, 4 H); H_p, 6.42 (t, J = 7.3 Hz, 2 H), H_o, 5.77 (d, J = 7.6 Hz, 4 H). FABMS, *m/e*: 894, cluster, M^+. UV–vis (toluene) λ_{max}, nm (log ϵ): 311 (4.37), 422 (5.17), 526 sh (4.02), 540 (4.08), 625 (3.75). Anal. Calcd for $C_{62}H_{46}N_4W$: C, 72.23; H, 4.50; N, 5.43. Found: C, 72.20; H, 4.39; N, 5.50.

W^{II}(OEP)$(PEt_3)_2$ (6). PEt_3 (4 mL) was vacuum-transferred into a conical Schlenk flask (10 mL) containing **2** (1.200 g, 1.52 mmol), Al(Hg) (1.0 g), and a stir bar. The suspension was degassed once via a freeze–pump–thaw cycle on a vacuum manifold (10^{-2} Torr). In a good fume hood and under a dry argon atmosphere, the suspension was heated at reflux for 44 h. The solution became homogeneous and a dark-orange color during this time. The solution was cooled and the excess phosphine vacuum-transferred into another flask. The orange–brown residue was heated under vacuum (60 °C, 10^{-2} Torr) for 5 h and then taken into the glovebox. The toluene-soluble products were extracted from the residue and flash chromatographed (SiO_2, 2 × 8 cm, toluene). The orange band was concentrated (3 mL), heated to redissolve the solid, and cooled, and then CH_3OH (5 mL) was carefully layered over the solution to crystallize the product. Filtration afforded lustrous black crystals which were washed with CH_3OH and dried under vacuum overnight (1.045 g, 72%). ^1H NMR (C_6D_6, ppm): H_{meso}, 18.11 (s, 4 H); CH_2CH_3, 2.37 (br q, 16 H); CH_2CH_3, –6.43 (br t, 24 H). ^3H NMR (C_6D_6, ppm), phosphine: CH_2CH_3, 35.60 (br q, 12 H); CH_2CH_3, 46.66 (br t, 18 H). UV–vis (toluene) λ_{max}, nm (log ϵ): 305 (4.74), 313 sh (4.73), 372 (4.76) 457 (3.99), 474 (4.03), 492 sh (4.00), 568 (3.73), 690 (3.44), 712 (3.43), 777 (3.62). Anal. Calcd for $C_{48}H_{74}N_4P_2W$: C, 60.50; H, 7.83; N, 5.88. Found: C, 60.71; H, 7.91; N, 5.88. μ_{eff} (C_6D_6) = 3.0 ± 0.2 μ_B.

[Re^{II}(OEP)]$_2$ (7). Crystalline Re(OEP)$(PEt_3)_2$ (475 mg, 0.497 mmol) was dissolved in benzene (50 mL) and frozen quickly with a liquid nitrogen bath. Under vacuum (10^{-2} Torr), the solid solution was warmed

(7) All the low-valent rhenium porphyrin complexes reported in the literature are univalent (6a–c) and a purported trivalent (6f) rhenium tricarbonyl "sitting atop" compounds coordinated to three of the four pyrrolic nitrogens of the porphyrin ligand. (a) Ostfeld, D.; Tsutsui, M.; Hrung, C. P.; Conway, D. C. *J. Am. Chem. Soc.* **1971**, *93*, 2548. (b) Cullen, D.; Meyer, E. F., Jr.; Srivastava, S.; Tsutsui, M. *J. Am. Chem. Soc.* **1972**, *94*, 7603. (c) Ostfield, D.; Tsutsui, M.; Hrung, C. P.; Conway, D. C. *J. Coord. Chem.* **1972**, *2*, 101. (d) Hrung, C. P.; Tsutsui, M. *J. Am. Chem. Soc.* **1973**, *95*, 5777. (e) Tsutsui, M.; Hrung, C. P.; Ostfeld, D.; Srivastava, T. S.; Cullen, D. L.; Meyer, E. F., Jr. *J. Am. Chem. Soc.* **1975**, *97*, 3952. (f) Kato, S.; Tsutsui, M.; Cullen, D. L.; Meyer, E. F., Jr. *J. Am. Chem. Soc.* **1977**, *99*, 620.

(8) Schumann, H. *J. Organomet. Chem.* **1985**, *290*, C34.

(9) Anker, M. W.; Colton, R.; Tomkins, I. B. *Aus. J. Chem.* **1967**, *20*, 9.

(10) Collman, J. P.; Garner, J. M.; Kim, K.; Ibers, J. A. *Inorg. Chem.* **1988**, *27*, 4513.

(11) Fuhrhop, J. H.; Smith, K. M. *Porphyrins and Metalloporphyrins*; Smith, K. M., Ed.; Elsevier: New York, 1975; p 769.

(12) Buchler, J. W.; Puppe, L.; Rohbock, K.; Schneehage, H. H. *Chem. Ber.* **1973**, *106*, 2710.

(13) Perrin, D. F.; Armarego, W. L. F.; Perrin, D. R. *Purification of Laboratory Chemicals*, 2nd ed.; Pergamon Press: New York, 1980; p 250.

(14) (a) Baker, M. V.; Field, L. D.; Hambley, T. N. *Inorg. Chem.* **1988**, *16*, 2872. This paper gives the Evans equation for a NMR spectrometer with a superconducting magnet. (b) Eaton, S. S.; Eaton, G. R. *Ibid.* **1980**, *19*, 1095. (c) Jolly, W. L. *The Synthesis and Characterization of Inorganic Compounds*; Prentice-Hall: Englewood Cliffs, NJ, 1970; p 371.

(15) Fleischer, E. B.; Chapman, R. D.; Krishnamurthy, M. *Inorg. Chem.* **1979**, *18*, 2156.

to 0 °C and the benzene sublimed away, yielding $Re(OEP)(PEt_3)_2$ as an amorphous orange powder. This air-stable solid was added to a pyrolysis tube and heated under vacuum (210 °C, 10^{-6} Torr) for 24 h. The orange solid turned blue–brown. The pyrolysis tube was isolated from the vacuum manifold and taken into a glovebox. The loose solid was separated from a small amount of $Re(OEP)(PEt_3)_2$ sublimate. Prepared in this manner, the product (340 mg, 95%) was analytically pure. FABMS, *m/e*: 1438, cluster, M^+. Anal. Calcd for $C_{72}H_{88}N_8Re_2$: C, 60.14; H, 6.17; N, 7.79. Found: C, 60.03; H, 6.24; N, 7.84.

$[Re^{II}(TTP)]_2$ (8). A yellow amorphous powder of $Re(TTP)(PEt_3)_2$ (32.5 mg, 0.0297 mmol) was prepared by the lyopholization procedure described for **7**. This solid was added to a pyrolysis tube and heated with a sand bath in an heating mantle under vacuum (300 °C, 10^{-6} Torr) for 5 h. The brown product (23.5 mg, 92%) was isolated as described for **7**. FABMS, *m/e*: 1710, cluster, M^+. UV–vis (toluene) λ_{max}, nm (log ϵ): 319 (4.08), 415 (4.78), 530 (3.63), 620 (3.38). Anal. Calcd for $C_{96}H_{72}N_8Re_2$: C, 67.43; H, 4.24; N, 6.55. Found: C, 67.80; H, 4.38; N, 6.50.

$[W^{II}(OEP)]_2$ (9). Method A. An orange–brown amorphous powder of **6** (300 mg, 0.315 mmol) was prepared by the lyopholization procedure described for the analogous $Re(OEP)(PEt_3)_2$ complex in the synthesis of **7**. This air-sensitive solid was then added to a pyrolysis tube and heated under vacuum (200 °C, 10^{-6} Torr) for 48 h. The pyrolysis tube was isolated from the vacuum manifold and taken into a glovebox. The loose solid was separated from a small amount of sublimate and was dissolved in hot toluene (200 mL), filtered through a glass wool plug, and then concentrated under vacuum (5 mL). The purple–blue crystals were collected by filtration, washed with hexanes (3 mL), and dried under vacuum. The product crystallizes with a 1/1 toluene solvate as determined by ^1H NMR. Yield: 255 mg, 78%. Anal. Calcd for $C_{79}H_{96}N_8W_2$: C, 62.21; H, 6.34; N, 7.35. Found: C, 62.01; H, 6.30; N, 7.55.

Method B. A benzene solution (10 mL) of **4** (190 mg, 0.212 mmol) was lyopholized to yield an air-sensitive purple powder. This solid was added to a pyrolysis tube and heated under vacuum (215 °C, 10^{-6} Torr) for 12 h. The pyrolysis tube was isolated from the vacuum manifold and taken into a glovebox. The starting material which sublimed partially up the tube was washed down with benzene (5 mL) into the bottom of the tube. This solution was again lyopholized and heated under vacuum (215 °C, 10^{-6} Torr) for another 12 h. This solid was purified as described in method A (162 mg, 89%). Anal. Calcd for $C_{79}H_{96}N_8W_2$: C 62.21; H, 6.34; N, 7.35. Found: C, 62.42; H, 6.40; N, 7.40.

Method C. Under scrupulously oxygen-free and anhydrous conditions, H_2OEP (26 mg, 0.047 mmol) and proton sponge (100 mg, 0.47 mmol) were dissolved in warm toluene (12 mL). $[W(CO)_4(Cl)_2]_2$ (150 mg, 0.41 mmol) was added, and the mixture was heated at reflux for 20 h. If H_2OEP was detected by TLC (Al_2O_3, toluene), another aliquot of $[W(CO)_4(Cl)_2]_2$ was added and heating continued until no free-base porphyrin remained. The cooled reaction mixture was filtered and flash chromatographed (Al_2O_3, 1 × 4 cm, toluene). The first brown band crystallized from toluene/hexanes to produce lustrous, dark blue microcrystals (1 mg, 3% based on porphyrin). FABMS (sulfolane), *m/e*: 1433, cluster, M^+. UV–vis (toluene) λ_{max}, nm (log ϵ): 379 (4.98), 431 (4.49), 562 (3.80).

$\{[Re^{II,III}(OEP)]_2\}(BF_4)\cdot C_6H_5CH_3$ (10). $[(Cp)_2Fe](BF_4)$ (5.7 mg, 0.021 mmol) was dissolved in CH_3CN (0.1 mL) and added dropwise to a rapidly stirred solution of **7** (30.4 mg, 0.0211 mmol) in toluene (1.5 mL). The solution was stirred for 1 h and the precipitate collected by filtration and washed with toluene (2 mL). This product crystallized from CH_2Cl_2/toluene as red–brown microcrystals which were dried under vacuum overnight (28.5 mg, 90%). ^1H NMR ($CDCl_3$, ppm): H_{meso}, not observed; CH_2CH_3, 6.25 (br s, 8 H); CH_2CH_3, 5.09 (br s, 8 H); CH_2CH_3 2.27 (br s). ^1H NMR ($CDCl_3$, ppm), solvate: $C_6H_5CH_3$, 7.28–7.14 (m, 5 H); $C_6H_5CH_3$, 2.35 (s). Anal. Calcd for $C_{79}H_{96}N_8BF_4Re_2$: C, 58.68; H, 5.98; N, 6.93. Found: C, 58.26; H, 5.77; N, 7.00. μ_{eff} ($CDCl_3$) = 1.7 ± 0.3 μ_B.

$\{[Re^{III}(OEP)]_2\}(BF_4)_2\cdot 1.5C_6H_5CH_3$ (11). A solution of **7** (30.0 mg, 0.0209 mmol) in toluene (1.5 mL) was added dropwise to a stirred solution of $AgBF_4$ (12.0 mg, 0.0616 mmol) dissolved in toluene (1 mL). The solution was stirred for 1 h and then the olive green precipitate was collected by filtration and washed with toluene (2 mL). This solid was dissolved in CH_2Cl_2 and filtered through a Celite pad to remove the silver metal. The brown filtrate was concentrated (2 mL) and then crystallized with the addition of toluene. The dark-green microcrystals were collected by filtration, washed with toluene, and dried under vacuum (32 mg, 91%). ^1H NMR (CD_2Cl_2, ppm): H_{meso}, 9.87 (s, 4 H); CH_2CH_3, 4.86 (m, 8 H); CH_2CH_3, 4.36 (m, 8 H); CH_2CH_3, 1.66 (t, J = 7.5 Hz, 24 H). ^1H NMR ($CDCl_2$, ppm), solvate: $C_6H_5CH_3$, 7.22–7.05 (m); $C_6H_5CH_3$, 2.32 (s, 2.25 H). Anal. Calcd for $C_{82.5}H_{100}N_8B_2F_8Re_2$: C, 56.63; H, 5.76; N, 6.40. Found: C, 56.49; H, 5.63; N, 6.61.

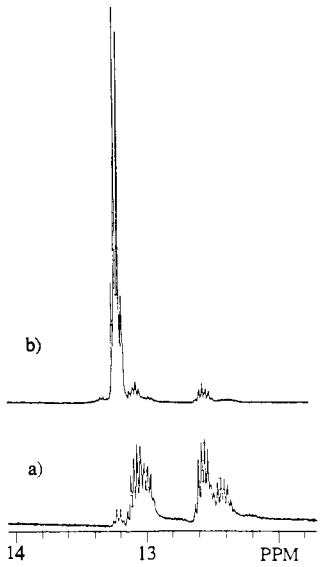

Figure 1. (a) Methylene ^1H NMR resonances of the reaction products after treating W(OEP)(O)(Cl) with Si_2Cl_6. (b) Methylene ^1H NMR resonances after treating the same reaction products with anhydrous HCl(g).

Table I. Chemical Shift Data for the $M^{IV}(Por)(Cl)_2$ Complexes in $CDCl_3$

	M(OEP)(Cl)$_2$			M(TTP)(Cl)$_2$			
					aryl		
M	H_{meso}	CH_2	CH_3	H_β	H_a	H_b	CH_3
Mo	−3.70	14.64	3.26	17.54	10.06	7.76	2.46
W	0.07[a]	13.25[b]	2.90[c]	14.38[d]	9.08[e]	8.03[f]	2.69[g]

[a] (s, 4 H). [b] (q, J = 7.1 Hz, 16 H). [c] (t, J = 7.2 Hz, 24 H). [d] (s, 8 H). [e] (d, J = 7.6 Hz, 8 H). [f] (d, J = 7.4 Hz, 8 H). [g] (s, 12 H).

Results and Discussion

Literature procedures for the synthesis of rhenium and tungsten porphyrin complexes yield metal(V) complexes with a metal–oxo multiple bond.[12] The other monoanionic ligand (methoxide, phenoxide, halide, etc.) can be varied easily due to the strong trans labilizing influence of the oxo ligand.

$W^{IV}(Por)(Cl)_2$. Replacement of the oxo ligand from the starting tungsten complex with chloride ligands results in a compound that can be reduced to yield low-valent tungsten porphyrin complexes. An oxophilic reagent that cleanly accomplishes this reaction under mild conditions is Si_2Cl_6. Treatment of the $W^V(Por)(O)(Cl)$ complexes with this reagent at 20 °C over the course of a few hours yields a mixture of paramagnetic $W^{IV}(Por)(X)(X')$

$$W^V(Por)(O)(Cl) \xrightarrow[CH_2Cl_2]{Si_2Cl_6} \xrightarrow[CH_2Cl_2]{HCl(g)} W^{IV}(Por)(Cl)_2 \quad (1)$$

Por = OEP, **2**; TTP, **3**

complexes where X or X′ = Cl^-, Cl_3Si^-, and Cl_3SiO^- as determined by mass spectroscopy and ^1H NMR. The reaction proceeds more rapidly in CH_2Cl_2 than in toluene. The contact shifted methylene resonances of the W(OEP)(X)(X′) mixture are shown in Figure 1a. Three complexes or isomers are present in the reaction solution; the two major products have diastereotopic resonances, indicating either X ≠ X′ or both X and X′ are coordinated on the same side of the porphyrin ring. This mixture of products can be converted to $W^{IV}(Por)(Cl)_2$ by bubbling anhydrous HCl through the reaction solution. The diastereotopic methylene resonances collapse into a quartet (Figure 1b), indicating a trans arrangement of the two chloride ligands similar to the structurally characterized $Mo(Por)(Cl)_2$ complexes.[16] Similar ^1H NMR

(16) (a) Diebold, T.; Chevrier, B.; Weiss, R. *Angew. Chem., Int. Ed. Engl.* **1977**, *16*, 788. (b) Diebold, T.; Chevrier, B.; Weiss, R. *Inorg. Chem.* **1979**, *18*, 1193.

results were also observed for the TTP complex (**3**). The similarity in chemical shifts of the $W(Por)(Cl)_2$ and $Mo(Por)(Cl)_2$ resonances (Table I) is evidence for the tetravalent oxidation state for the tungsten compounds. The magnetic moments for the tungsten OEP and the TTP compounds are significantly lower than those reported for the $Mo^{IV}(Por)(Cl)_2$ complexes but are similar in magnitude to other six-coordinate W(IV) halide complexes with nitrogen or phosphorus donors (2.10–1.78 μ_B).[17] Hence, the net effect of treating the $W^V(Por)(O)(Cl)$ compounds with the Si_2Cl_6 reagent is to remove the oxo ligand and reduce the tungsten ion. The products were isolated as crude solids which are suitable for further reactions.

$W^{II}(Por)(H_5C_6C{\equiv}CC_6H_5)$. Tungsten porphyrin acetylene complexes have been prepared by a synthetic route similar to that used for the analogous molybdenum compounds.[1,18] A mistake in an organometallics text incorrectly reported that the tungsten compounds had been previously prepared.[19] The $W(Por)(Cl)_2$ complexes are reduced with $LiAlH_4$ in the presence of excess

$$W^{IV}(Por)(Cl)_2 + H_5C_6C{\equiv}CC_6H_5 \xrightarrow[C_6H_5CH_3,\ N_2]{LiAlH_4,\ THF} W^{II}(Por)(H_5C_6C{\equiv}CC_6H_5) \quad (2)$$

Por = OEP, **4**; TTP, **5**

diphenylacetylene to yield the diamagnetic 14-electron complexes. The reduction proceeds more rapidly and gives greater yields when $W(Por)(Cl)_2$ is added as a solid to the stirred suspension of $LiAlH_4$ and the acetylene in the toluene/THF solvent mixture. The ^1H NMR and visible electronic spectra of the tungsten OEP and TTP complexes are very similar to those of the analogous molybdenum compounds. These complexes are both acutely oxygen-sensitive when in solution.

A crystallographic study of $Mo(TTP)(H_5C_6C{\equiv}CC_6H_5)$ indicated the bonding between the molybdenum ion and the acetylene is best described as a metallocyclopropene structure with the acetylene ligand acting as a four-electron donor.[18] General periodic trends would predict that the tungsten acetylene complexes should also have metallocyclopropene structures, as higher oxidation states are more stable as one descends a triad and 5d metals tend to π-backbond to a greater extent with π-acid ligands than do the 3d and 4d metals.[20] Experimental evidence to support this trend would come from a comparison of the symmetric acetylenic carbon–carbon stretching frequencies of $Mo(TTP)(H_5C_6C{\equiv}CC_6H_5)$ and the tungsten TTP compound (**5**). These stretches become infrared active as the metal releases π-electron density (d_{xz} or d_{yz}) into the acetylene LUMO (π^*) forming the metallocyclopropene structure.[21] However, no IR bands between 2200 and 1700 cm^{-1} were observed for either of the molybdenum or tungsten complexes as KBr samples or fluorolube mulls. The intensities of these coordinated acetylene bands are evidently too weak to observe. The tungsten compounds add to a growing list of organotransition metal porphyrin complexes.[22]

$Re^{II}(Por)(PEt_3)_2$ and $W^{II}(OEP)(PEt_3)_2$. Earlier, we reported the synthesis of rhenium(II) porphyrin complexes with trans axial trimethyl- and triethylphosphine ligands.[10] These low-spin complexes ($\mu_{eff} = 1.6 \pm 0.2\ \mu_B$) are prepared in good yields by treating rhenium(V) porphyrin complexes with neat refluxing phosphine.

$$Re^V(Por)(O)(Cl) \xrightarrow[125\ °C,\ Ar]{PEt_3} Re^{II}(Por)(PEt_3)_2 \quad (3)$$

Por = OEP, TTP

A similar reaction with $W^V(Por)(O)(Cl)$ failed to produce any reduced species, but a divalent tungsten phosphine complex (**6**)

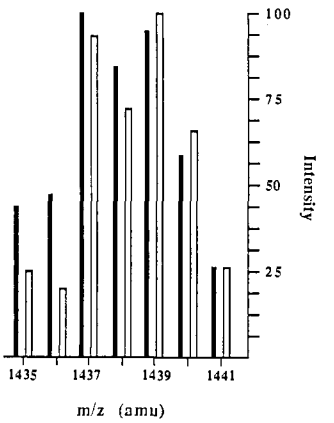

Figure 2. FAB mass spectrum of $[Re(OEP)]_2$. Experimental (■); calculated (□).

is the major product when $W^{IV}(OEP)(Cl)_2$ is reduced with Al(Hg) in boiling PEt_3. This product is not produced in the absence of

$$W^{IV}(OEP)(Cl)_2 \xrightarrow[125\ °C,\ Ar]{Al(Hg),\ PEt_3} \underset{\mathbf{6}}{W^{II}(OEP)(PEt_3)_2} \quad (4)$$

Al(Hg) under similar conditions, implicating aluminum as the reductant and not the phosphine. The reaction is carried out under high concentration conditions in order to minimize the hydrolysis of $W^{IV}(OEP)(Cl)_2$ with adventitious water. Elemental analyses and the ^1H NMR spectrum are consistent with two axially coordinated phosphine ligands. Even though **6** is paramagnetic, the five observed ^1H NMR resonances are not significantly broadened, and the spin–spin splitting patterns are easily recognized. Together with decoupling experiments and integration, each resonance can be correctly assigned. The porphyrin methylene resonance appears as a quartet, suggesting a plane of symmetry containing the porphyrin ligand and a solution structure with a trans arrangement of the axial phosphine ligands. An analogous molybdenum(II) phosphine complex has not been reported but *trans*-$Mo^{II}(TTP)(Py)_2$ has been prepared and structurally characterized.[23] The reported solid-state magnetic moment for this complex (2.80 μ_B) compares favorably with the solution value (3.0 ± 0.2 μ_B) measured for the tungsten OEP complex (**6**). Both are consistent with a low-spin, d^4 metal ions with two unpaired electrons. The latter value is slightly higher than the moments for other octahedral W(II) phosphine and arsine compounds (2.70–2.3 μ_B)[17] and may imply a mixing of the ground-state orbitals with an excited multiplet state.[24] A Curie-law dependence of the chemical shifts of the tungsten OEP complex in toluene (−90 to 90 °C) is observed, suggesting that a single spin state is present over the temperature range investigated. The tungsten phosphine complex is much more oxygen-sensitive, both in solution and the solid state, than the corresponding rhenium phosphine complexes.

$[Re^{II}(Por)]_2$ and $[W^{II}(OEP)]_2$. The rhenium phosphine complexes are suitable precursors to the rhenium(II) porphyrin dimers. The successful synthetic route employs the solid-state vacuum pyrolysis reaction developed earlier for the synthesis of the ruthenium and osmium porphyrin dimers.[1] The crystalline rhenium phosphine precursors are first converted to amorphous powders by a benzene lyophilization procedure. This procedure is employed to destroy virtually all of the solid crystalline domains, producing a porous, high surface area solid that permits the facile removal of the volatile axial phosphine ligands. Vacuum pyrolysis of these solids produces the highly oxygen-sensitive dimers in virtually quantitative yields. As observed for the syntheses of the ru-

$$2Re^{II}(Por)(PEt_3)_2 \xrightarrow[10^{-6}\ Torr]{\Delta} [Re^{II}(Por)]_2 \quad (5)$$

Por = OEP, 210 °C, **7**; TTP, 300 °C, **8**

(17) Dori, Z. *Prog. Inorg. Chem.* **1981**, *28*, 239.
(18) De Cian, A.; Colin, J.; Schappacher, M.; Ricard, L., Weiss, R. *J. Am. Chem. Soc.* **1981**, *103*, 1850.
(19) Collman, J. P.; Hegedus, L. S.; Norton, J. R.; Finke, R. G. *Principles and Applications of Organotransition Metal Chemistry*; University Science: Mill Valley, CA, 1987; p 185.
(20) Collman, J. P.; Hegedus, L. S. *Principles and Applications of Organotransition Metal Chemistry*; University Science: Mill Valley, CA, 1980; p 110.
(21) Otsuka, S.; Nakamura, A. *Adv. Organomet. Chem.* **1976**, *14*, 245.
(22) Brothers, P. J. Collman, J. P. *Acc. Chem. Res.* **1986**, *19*, 209.
(23) Colin, J.; Strich, A.; Schappacher, M.; Chevrier, B.; Veillard, A.; Weiss, R. *Nouv. J. Chim.* **1984**, 55.
(24) Drago, R. S. *Physical Methods in Chemistry*; W. B. Saunders: Philadelphia, PA, 1977; p 425.

Table II. Chemical Shift Data for the Neutral Dimetalloporphyrin Complexes in C_6D_6 at 21 °C

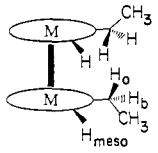

$[M^{II}(OEP)]_2$

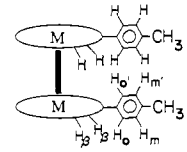

$[M^{II}(TTP)]_2$

M	H_{meso}	CH_2 H_a	H_b	CH_3	H_β	H_o	H_m	$H_{o'}$	$H_{m'}$	CH_3
Mo	9.20	4.32	3.92	1.78	8.85	7.09[a]		9.63	7.80	2.57
W	8.42	4.11	3.76	1.67						
Re	6.45	3.97	3.70	1.63	8.00	7.10	7.18	9.04	7.59	2.47
Rh	9.17	4.50	4.00	1.75	8.68	7.13	7.25	9.69	7.80	2.54
Ir	8.91	4.35	3.90	1.66						
Ru	10.14	25.51	11.0	3.42	−14.14	6.46	7.49	13.25	9.28	3.45
Os	−1.08	11.56	7.83	1.97	−1.19	6.01	7.52	9.70	8.52	3.11

[a] Both the H_o and H_m resonances overlap for the Mo dimer. The circles in the graphics represent the porphyrin macrocycle with substituents as indicated.

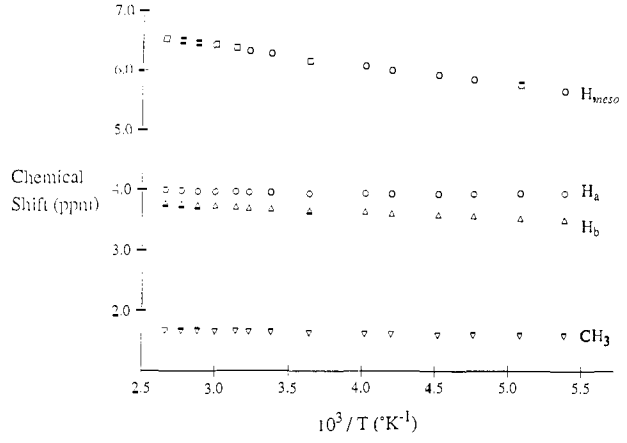

Figure 3. Temperature dependence of the ^1H NMR resonances of $[Re(OEP)]_2$ in $C_6D_5CD_3$ between −95 and 100 °C (TMS internal standard).

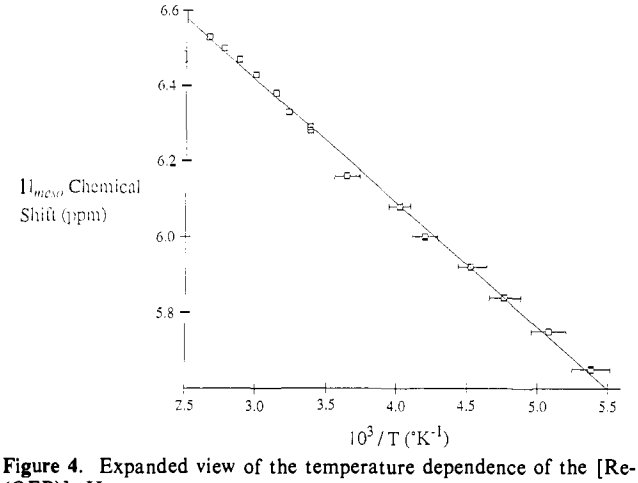

Figure 4. Expanded view of the temperature dependence of the $[Re(OEP)]_2$ H_{meso} resonance.

thenium and osmium dimers, higher temperatures are required for the TTP complex than the OEP complex, and side reactions resulting in other products are not observed. Elemental analyses are consistent with $[Re(Por)]_n$ formulations, and the most intense isotope clusters in the FAB mass spectra are those of the dinuclear complexes (Figure 2) with a very weak cluster corresponding to the monomer or the dimer dication. The ^1H NMR spectra indicate that both the OEP and TTP dimers possess 4-fold axial symmetry. The diastereotopic methylene resonances of the OEP dimer and the four chemically inequivalent doublets for the *p*-tolyl aryl resonances of the TTP dimer are both consistent with loss of the porphyrin plane of symmetry and slow rotation on the NMR time scale of the TTP aryl rings[25] which usually lie roughly perpendicular to this plane.[26] The chemical shifts and appearance of these resonances are virtually identical with those observed for the other diamagnetic porphyrin dimers as listed in Table II. An exception is the H_{meso} resonance of the OEP dimer. This resonance appears at 6.45 ppm in C_6D_6, which is approximately a 2.5 ppm shift upfield from the average value of H_{meso} for the other diamagnetic dimers. The chemical shift of this resonance is neither concentration nor solvent dependent.[27] However, the H_{meso} and methylene resonances for the OEP dimer are weakly temperature dependent in toluene, and a Curie plot of chemical shift versus T^{-1} yields straight lines, as shown in Figures 3 and 4. The range of chemical shifts for H_{meso} (Δppm ~ 0.9) is much greater than those of the two methylene resonances (Δppm ~ 0.07 and 0.27) over the same temperature range (−90 to +100 °C). Although the resonances of free-base porphyrins have been shown to have temperature dependencies comparable to the shifts observed for the $[Re(OEP)]_2$ methylene resonances,[28] the 0.9 ppm H_{meso} shift appears to be without precedent for a diamagnetic metalloporphyrin. In contrast, no unusual shifts of the rhenium TTP dimer are observed. Only modest deviations from the average chemical shift values for the diamagnetic $[Mo(TTP)]_2$ and $[Rh(TTP)]_2$ complexes are evident.

Paramagnetism associated with the rhenium–rhenium bond could possibly result in a contact shift of the H_{meso} resonance similar to the observed contact shifts for the paramagnetic ruthenium and osmium porphyrin dimers.[1,2] However, any paramagnetic explaination must also account for the fact that the H_{meso} resonance is contact shifted, whereas the ethyl group resonances are not. Two possible paramagnetic electronic configurations for two interacting d^5 rhenium ions can be predicted from the molecular orbital scheme[29a] (Figure 5). If the π^* orbitals are lower in energy than the δ^* orbital (or η in D_{4d} symmetry), a triplet electronic configuration ($\sigma^2\pi^4\delta^2\pi^{*1}\pi^{*1}$) could result. However, the magnetic moment for $[Re(OEP)]_2$ in solution (21 °C) is too low to measure by the Evans method, but it is estimated with the Evans equation that the μ_{eff} value must be ≤ 0.8 μ_B after correcting

(25) Eaton, S. S.; Eaton, G. R. *J. Am. Chem. Soc.* **1977**, *99*, 6594.
(26) (a) Scheidt, W. R.; Lee, Y. J. *Struct. Bonding (Berlin)* **1987**, *64*, 1. (b) Hoard, J. L. *Porphyrins and Metalloporphyrins*; Smith, K. M., Ed.; Elsevier: New York, 1975; p 317.
(27) ^1H NMR (C_6D_{12}, ppm): H_{meso}, 6.53 (s, 4 H); CH_2CH_3, 3.93 (m, 8 H); CH_2CH_3 3.70 (m, 8 H); CH_2CH_3 1.55 (t, J = 7.6 Hz, 24 H). Also, added $Re(OEP)(PEt_3)_2$ (a likely impurity in the $[Re(OEP)]_2$ synthesis) over the concentration range of 1–10 mol % has no detectible influence upon the chemical shift of the $[Re(OEP)]_2$ H_{meso} resonance.
(28) Janson, T. R.; Katz, J. J. *The Porphyrins*; Dolphin, D., Ed.; Academic Press: San Francisco, CA, 1979; Vol. IV, p 17.

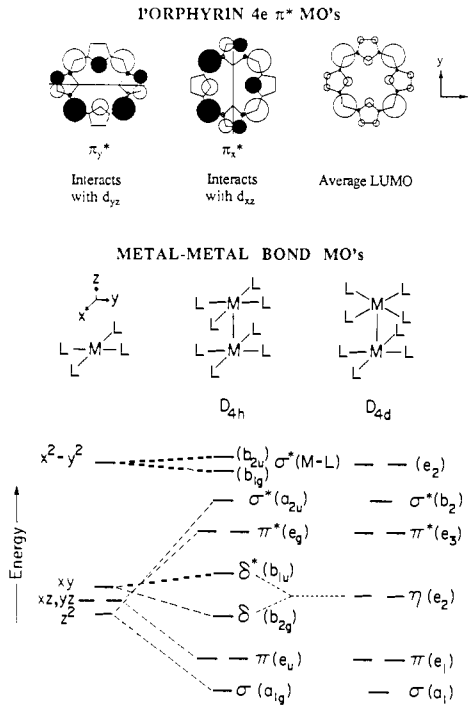

Figure 5. Metal–metal bonding MO diagram for a M_2L_8 complex and the porphyrin 4e π^* orbitals. The circles can represent the top lobes of $2p_z$ atomic orbitals, and the size of each is proportional to the square of the coefficient for that particular orbital in the MO.

for ligand diamagnetism. This upper limit is probably sufficiently accurate to rule out the triplet ground state. In fact, this measurement strongly suggests a diamagnetic ground state, $[\sigma^2\pi^4\delta^2\delta^{*2}$ (D_{4h}) or $\sigma^2\pi^4\eta^4$ $(D_{4d})]$. Assuming this is true, a paramagnetic contribution to this diamagnetic ground state would result if the metal–metal δ^* and π^* orbitals are close in energy. A populated excited state, $\sigma^2\pi^4\delta^2\delta^{*1}\pi^{*1}(D_{4h})$ or $\sigma^2\pi^4\eta^3\pi^{*1}$ (D_{4d}), would place unpaired spin density within a metal–metal bonding orbital (π^*) capable of interacting with the lowest unoccupied porphyrin orbital of E symmetry (4e π^*) via backbonding. This porphyrin wave function[29b,c] (Figure 5) would distribute the majority of any delocalized unpaired spin density at the meso carbon of the porphyrin ligand and a smaller portion at the β-pyrrolic carbons where the ethyl groups are positioned. Hence, the H_{meso} resonance might be expected to experience a greater contact shift than the methylene resonances simply because there should be greater unpaired spin density at the meso carbon than at the β-pyrrolic carbon. This same type of delocalization into the porphyrin 4e π^* orbital is attributed to be the dominate mechanism for the contact shifts in $[Os(OEP)]_2$ where a larger upfield shift of the H_{meso} resonance is observed.[30] If this same type of delocalization is occurring for $[Re(OEP)]_2$, one might have also expected a small downfield shift of the β-pyrrolic methylene resonance,[29b,30] but this is not observed. In fact, as the temperature is lowered, both of the methylene resonances shift upfield, as does the H_{meso} resonance.

We have also prepared another rhenium porphyrin dimer similar to the OEP dimer where each porphyrin is substituted at a single meso position with a phenyl group; the other three meso positions are unsubstituted.[31] This complex exhibits two H_{meso} resonances. The two-proton resonance appears at 6.87 ppm, similar to the H_{meso} chemical shift for $[Re(OEP)]_2$, and the one-proton resonance appears at 8.12 ppm, closer to the average H_{meso} chemical shift for the diamagnetic dimers. These observations nicely fit the excited-state explanation. The phenyl group may be able to interact with the porphyrin π orbitals sufficiently to remove the degeneracy at the meso carbons for the average porphyrin 4e π^* orbital, resulting in unequal unpaired spin density at the two different types of unsubstituted meso carbons. This should result in two different H_{meso} chemical shifts, as is observed.

Another interesting aspect of this excited-state postulate is that the energy of the metal–metal δ^* orbital varies as the two macrocycles rotate with respect to each other. The δ-bonding interaction is angle-dependent.[32] These bonds result from overlap between the two d_{xy} atomic orbitals and overlap varies as cos 2χ (χ is the N–Re–Re–N dihedral angle away from the perfectly eclipsed conformation). However, the metal–metal π-bonding interactions are not angle-dependent due to their combined cylindrical symmetry, much like the π-electron density in an acetylene. Experimental estimates of the η to δ^* energy separation in molybdenum complexes are approximately 10 times the thermal energy available at room temperature.[3,33] Therefore, depending upon this energy separation for $[Re(OEP)]_2$, only certain conformations (i.e., eclipsed or nearly eclipsed) should have a thermally populated excited state. Isoelectronic diosmium tetracarboxylate complexes $[Os^{III}_2(O_2CR)_4Cl)_2]$, where the bridging carboxylate ligands require an eclipsed conformation, are reported to have magnetic moments that decrease with decreasing temperature, suggesting a thermal equilibrium between two different spin states.[34]

However, these solution NMR observations are not strong evidence for an equilibrium between singlet–triplet spin states in $[Re(OEP)]_2$ especially since the Curie plot of chemical shift versus T^{-1} is linear. Furthermore, solid-state magnetic susceptibility measurements between 2 and 320 K indicate $[Re(OEP)]_2$ is a simple diamagnet. The data can be fitted by assuming a $S = {}^1/_2$ Curie impurity [presumably $Re^{II}(OEP)(PEt_3)_2$] is also present. However, the solid-state result may simply reflect differences in structural and dynamic properties of $[Re(OEP)]_2$ in solution and the solid, which leads to different magnetic properties in each phase. MCD measurements are probably the only other experimental method to investigate whether excited electronic states are actually populated in solution. Two other explanations that do not rely on a paramagnetic contact shift mechanism may also be considered: (a) intramolecular porphyrin–porphyrin interactions may result in increased shielding at the meso carbon of $[Re(OEP)]_2$, which is absent in the other diamagnetic dimers; (b) magnetic anisotropy associated with the rhenium–rhenium multiple bond[35] may influence the chemical shift of H_{meso}. However, it is difficult to account for the temperature dependence of the H_{meso} chemical shift with these explanations.

The $[W^{II}(OEP)]_2$ complex (**9**) can be prepared by three different methods. Both the tungsten octaethylporphyrin acetylene (**4**) and phosphine (**6**) complexes are precursors to this dimer via the solid-state pyrolysis reaction described for the rhenium

(29) (a) Cotton, F. A.; Curtis, N. F.; Harris, C. B.; Johnson, B. F. G.; Lippard, S. J.; Mague, J. T.; Robinson, W. R.; Wood, J. S. *Science* **1964**, *145*, 1305. Cotton, F. A. *Inorg. Chem.* **1964**, *4*, 334. (b) La Mar, G. N.; Walker (Jensen), F. A. *The Porphyrins*; Dolphin, D., Ed.; Academic Press: San Francisco, CA, 1979; Vol. IV, p 61. (c) Longuet-Higgins, H. C.; Rector, J. R.; Platt, J. R. *J. Chem. Phys.* **1950**, *18*, 1174.

(30) Barnes, C. E. Ph.D. Thesis, Stanford University, Stanford, CA, 1983. This explanation ignores any dipolar contributions to the observed H_{meso} shift. Also, the metal–metal δ^* orbital is orthogonal to all the porphyrin orbitals, and any unpaired electron density within this orbital cannot be delocalized into any of the porphyrin orbitals, so its contribution to the contact shift of H_{meso} has been ignored in this discussion.

(31) Bis[(5-(4-methoxyphenyl)-2,3,7,8,13,17-hexaethyl-12,18-dimethylporphyrin)rhenium(II)]. ^1H NMR ($C_6D_5CD_3$, ppm, 21 °C): $H_{o'}$, 8.82 (d, J = 8.2 Hz, 1 H), $H_{m'}$, 7.54 (d, J = 7.2 Hz, 1 H); H_o (−25 °C), 6.90 (d, J = 8.3 Hz); H_m, 6.72 (d, J = 7.7 Hz, 1 H); CH_2CH_3, 4.25–3.95 (m, 4 H); CH_2CH_3, 3.90–3.55 (overlapping m); CH_2CH_3, 3.05–2.90 (m, 2 H); CH_2CH_3, 2.60–2.40 (m, 2 H); CH_3, 3.79 (overlapping s); OCH_3, 3.63 (overlapping s); CH_2CH_3, 1.62 (t, J = 6.7 Hz, 12 H); CH_2CH_3 1.29 (t, J = 6.0 Hz, 6 H). FABMS (sulfolane), m/e: 1594, cluster, M^+.

(32) Cotton, F. A.; Fanwick, P. E.; Fitch, J. W.; Glicksman, H. D.; Walton, R. A. *J. Am. Chem. Soc.* **1979**, *101*, 1752.

(33) Hopkins, M. D.; Zietlow, T. C.; Miskowski, V. M.; Gray, H. B. *J. Am. Chem. Soc.* **1985**, *107*, 510.

(34) (a) Stephenson, T. A.; Tocher, D. A.; Walkinshaw, M. D. *J. Organomet. Chem.* **1982**, *232*, C51. (b) Behling, T.; Wilkinson, G.; Stephenson, T. A.; Tocher, D. A.; Walkinshaw, M. D. *J. Chem. Soc., Dalton Trans.* **1983**, 2109.

(35) Chisholm, M. H.; Cotton, F. A.; Frenz, B. A.; Reichert, W. W.; Shive, L. W.; Stults, B. R. *J. Am. Chem. Soc.* **1976**, *98*, 4469. Blatchford, T. P.; Chisholm, M. H.; Folting, K.; Huffman, J. C. *Inorg. Chem.* **1980**, *19*, 3175.

phosphine complexes. The tungsten reactions are shown in eq 6 and 7. The acetylene complex is quite thermally robust, as it

$$2W^{II}(OEP)(H_5C_6C{\equiv}CC_6H_5) \xrightarrow[10^{-6}\ Torr]{215\ °C} [W^{II}(OEP)]_2 \quad (6)$$

$$2W^{II}(OEP)(PEt_3)_2 \xrightarrow[10^{-6}\ Torr]{200\ °C} [W^{II}(OEP)]_2 \quad (7)$$

requires two sequential lyopholization/pyrolysis procedures for the reaction in eq 6 to reach completion in high yield. A significant portion of the starting material simply sublimes at 215 °C during the first pyrolysis. Phosphine dissociation in eq 7 is facile at 210 °C, but elemental analyses of the pyrolysis solid suggest that it is contaminated with other unidentified products. Lowering the temperature of this reaction appears to minimize the formation of these byproducts, and purification by crystallization yields an analytically pure product. The tungsten dimer is significantly less soluble and more oxygen-sensitive than the other dimetalloporphyrin complexes. The ^{1}H NMR spectrum is consistent with a diamagnetic dimer, and an intense molecular ion for $[W(OEP)]_2$ is observed in the FAB mass spectrum with an air-sensitive handling technique. The visible electronic spectrum also resembles that of the $[Mo(OEP)]_2$ complex very closely.[1] The synthesis of the tungsten TTP dimer was not investigated.

Another method for the synthesis of $[W(OEP)_2]$ is patterned after the single-step synthesis of the $[Mo(OEP)]_2$ complex.[3] Under rigorously anaerobic and anhydrous conditions, $[W^{II}(CO)_4(Cl)_2]_2$ and free-base OEP in refluxing toluene yields a product that by

$$[W^{II}(CO)_4(Cl)_2]_2 + H_2OEP \xrightarrow[\text{proton sponge}]{C_6H_5CH_3,\ 110\ °C,\ N_2} [W^{II}(OEP)]_2 \quad (8)$$

UV-vis and ^{1}H NMR is identical with the product prepared by the solid-state reactions above. However, the yield is very poor (3%), and the largest successful scale yields only 1 mg of product. Attempts to modify the reaction conditions (i.e., different solvents, bases, metal sources) to improve the yield or scale were unsuccessful. Of all three methods for the synthesis of $[W(OEP)]_2$, method A is preferred because of the greater stability and ease of handling the tungsten phosphine precursor complex (**6**).

$\{[Re(OEP)]_2\}^{1+}$ and $\{[Re(OEP)]_2\}^{2+}$. Recently, we reported both the electrochemical and chemical redox properties of $[Ru(OEP)]_2$ and $[Os(OEP)]_2$. These complexes were shown to undergo two metal-centered oxidations to form cationic complexes while retaining their dimeric structures.[36] These oxidations allow the metal–metal bond order to be increased by removing antibonding electron density from this bond. The $[Re(OEP)]_2$ complex can also be oxidized with mild, single-electron, outer-sphere oxidants, such as $[(Cp)_2Fe^{III}]^+$ or Ag^+ in toluene, to yield two different products dependent upon the reaction stoichiometry as shown in eq 9 and 10. The yields for both reactions are 90% or better.

$$[Re^{II}(OEP)]_2 + [(Cp)_2Fe^{III}](BF_4) \xrightarrow{C_6H_5CH_3} \underset{\mathbf{10}}{\{[Re^{II,III}(OEP)]_2\}(BF_4)} \quad (9)$$

$$[Re^{II}(OEP)]_2 + 2AgBF_4 \xrightarrow{C_6H_5CH_3} \underset{\mathbf{11}}{\{[Re^{III}(OEP)]_2\}(BF_4)_2} \quad (10)$$

Satisfactory elemental analyses support the formulations given for the products. The product (**10**) of eq 9 gives a broadened ^{1}H NMR spectrum due to the paramagnetism, but two different signals are still observed for the methylene resonances, as shown in Figure 6b. This strongly supports diastereotopic methylene resonances, indicating a dimeric structure for the complex. The magnetic moment ($1.7 \pm 0.3\ \mu_B$) for **10** is consistent with one unpaired electron per dimer complex as would be expected for a low-spin, mixed valence dirhenium complex with a $\sigma^2\pi^4\delta^2\delta^{*1}$ electronic configuration. A good X-ray diffraction data set was

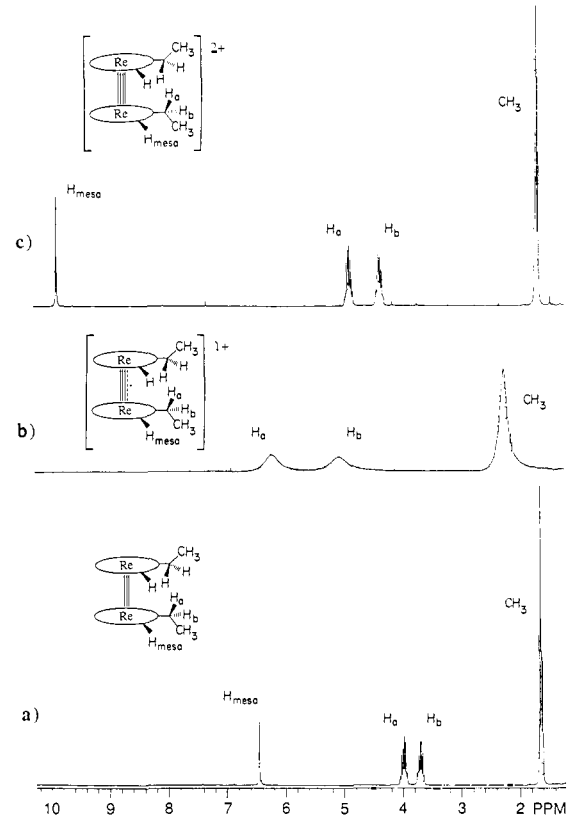

Figure 6. ^{1}H NMR spectra of dimeric rhenium porphyrins: (a) $[Re(OEP)]_2$ in C_6D_6; (b) $\{[Re(OEP)]_2\}(BF_4)$ in $CDCl_3$; (c) $\{[Re(OEP)]_2\}(BF_4)_2$ in CD_2Cl_2. Solvent and toluene solvate resonances have been omitted.

Table III. UV-Visible Bands for the $\{[Re(OEP)]_2\}^{n+}$ Complexes[a]

complex	Soret region	lower energy bands
$n = 0$[b]	354 (4.67), 405 (4.99)	464 sh[d] (4.10), 498 (4.00), 536 sh (3.89), 580 (3.71), 622 (3.70), 646 (3.70)
$n = 1$[c]	322 sh (4.59), 354 (4.69), 395 (4.94)	456 sh (4.17), 517 (3.86), 576 sh (3.57), 684 (3.41)
$n = 2$[c]	350 (4.85), 393 (4.66)	462 sh (4.14), 680 (3.33)

[a] Each band is represented as λ_{max}, nm (log ϵ). [b] Toluene. [c] CH_2Cl_2. [d] sh = shoulder.

obtained for a single crystal of **10** grown from CH_2Cl_2/toluene. However, two different disordered solvate molecules within the unit cell resulted in an unsolvable crystal structure.[37] The ^{1}H NMR spectrum (Figure 6c) of the product (**11**) in eq 10 is similar to the other diamagnetic dimers, and the chemical shifts are virtually identical with those of the dicationic ruthenium and osmium OEP dimers. These data are consistent with the predicted $\sigma^2\pi^4\delta^2$ electronic configuration for a metal-centered oxidation.

Although it is somewhat naive to suggest the porphyrin ligand would be oxidized before the rhenium–rhenium bond, none of the evidence in the preceding paragraph is inconsistent with these oxidations generating dimeric complexes with porphyrin π-radical cations. However, monomeric metalloporphyrin π-radical cations have been isolated and studied by others, and several spectroscopic criteria can be used to differentiate metal versus porphyrinic oxidations. A ligand-centered oxidation for metalloporphyrins results in a blue shift of the Soret absorption ($\pi \rightarrow \pi^*$) accompanied by broadening and a decrease in the extinction coefficient.[38]

(36) Collman, J. P.; Prodolliet, J. W.; Leidner, C. R. *J. Am. Chem. Soc.* **1986**, *108*, 2916.

(37) Collman, J. P.; Garner, J. M.; Kim, K.; Ibers, J. I. Unpublished results. Two nuclei separated by 2.3 Å could be determined from the diffraction pattern, which is consistent with a Re–Re distance of bond order 3.5 or a typical Re–Cl distance.

(38) (a) Fuhrhop, J.-H. *Struct. Bonding (Berlin)* **1974**, *18*, 1. (b) Fuhrhop, J.-H. *Porphyrins and Metalloporphyrins*; Smith, K. M., Ed.; Elsevier: New York, 1976; p 609.

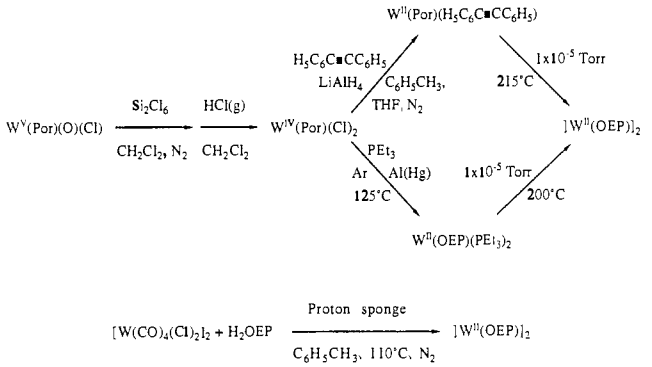

Figure 7. Coordination chemistry of low-valent tungsten porphyrin complexes.

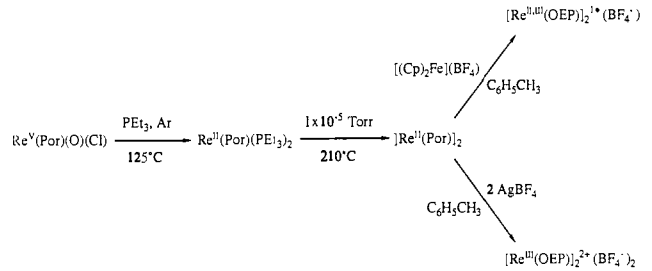

Figure 8. Coordination chemistry of low-valent rhenium porphyrin complexes.

Also, a prominent visible band above 600 nm is often observed. A blue shift of the Soret bands is observed for the mono- and dicationic rhenium dimers (Table III), but the band intensities are not diminished in comparison to the neutral rhenium dimer nor are any strong absorptions above 600 nm observed. A similar blue-shifted Soret was also observed for the cationic ruthenium and osmium dimers.[36] Metalloporphyrin π-radical cations also exhibit a strong infrared absorption near 1560 cm^{-1} for the OEP macrocycle,[39] but again no strong bands in this region are observed for both cationic rhenium OEP dimers. Furthermore, a complete resonance Raman and infrared vibrational study of the dimeric metalloporphyrins with metal–metal multiple bonds (11 complexes) indicates the porphyrin skeletal vibrations of the cationic rhenium OEP dimers are virtually identical with the other dimeric metalloporphyrins,[40] including the neutral rhenium dimer, which is inconsistent with ligand-centered oxidations.

Conclusions

The coordination chemistry of low-valent rhenium and tungsten porphyrin complexes developed in this study is summarized in Figures 7 and 8. $W^{IV}(Por)(Cl)_2$, $W^{II}(Por)(H_5C_6C{\equiv}CC_6H_5)$, and $W^{II}(OEP)(PEt_3)_2$ were found to be similar to the analogous molybdenum porphyrin complexes by spectroscopic and magnetic measurements. The tungsten acetylene and phosphine complexes are suitable precursors to the diamagnetic, quadruply bonded $[W^{II}(OEP)]_2$ complex via the solid-state vacuum pyrolysis reaction previously developed for the $[Ru^{II}(Por)]_2$, $[Os^{II}(Por)]_2$, and $[Mo^{II}(Por)]_2$ complexes. The triply bonded $[Re^{II}(Por)]_2$ compounds were prepared by a similar pyrolysis reaction of the $Re^{II}(Por)(PEt_3)_2$ compounds. Population of a paramagnetic excited state for $[Re^{II}(OEP)]_2$ has been postulated based upon an unusual chemical shift and temperature dependence of the H_{meso} resonance. However, no other evidence to support this postulate is found in solution, and solid-state magnetic measurements indicate this dimer is diamagnetic. $[Re^{II}(OEP)]_2$ can be oxidized to yield mono- and dicationic dimeric complexes. UV–visible and vibrational spectroscopies indicate that these oxidations occur at the metal–metal bond rather than the porphyrin ligand.

Earlier, we proposed that the formation of strong metal–metal bonds between metalloporphyrins for the 4d and 5d transition metals might be a general phenomenon. With the addition of the rhenium and tungsten compounds, 13 metallooctaethylporphyrin dimers have been prepared, including the cationic species. These interesting compounds presently represent the largest class of isostructural metal complexes with M_2L_8 structures and span a wide range of metals, valence d electron counts, and bond orders. Many exciting opportunities arise to study systematically the structural, spectroscopic, and chemical properties within this family of compounds. For example, the same dynamic ^1H NMR experiments used to determine the rotational barrier in the molybdenum(II) dimer can now be applied to the rhenium(III) and tungsten(II) dimers. This would allow a direct comparison of the relative δ bond strengths of these isostructural complexes. Preliminary results indicate that a rotational barrier for the tungsten dimer is observable and the activation energy will be surprising to many researchers in this subfield of inorganic chemistry.

Acknowledgment. This work was supported by the National Science Foundation (CHE83-18512). The NMR instrument used is supported by an NSF grant (CHE81-09064). We are thankful to Drs. J. Leary and E. Tolun at the UC—Berkeley mass spectrometry laboratory for their efforts in developing an inert-atmosphere FABMS technique for the analysis of these new compounds. Dr. Joel Miller (Du Pont Central Research) is thanked for the solid-state magnetic susceptibility measurements of $[Re(OEP)]_2$. This work is dedicated to J.M.G.'s father, James H. Garner.

(39) Shimomura, E. T.; Phillippi, M. A.; Goff, H. M.; Scholz, W. F.; Reed, C. A. *J. Am. Chem. Soc.* **1981**, *103*, 6778.

(40) Tait, C. D.; Garner, J. M.; Sattelberger, A. P.; Collman, J. P.; Woodruff, W. H. *Abstracts of Papers*, 196th National Meeting of the American Chemical Society, Los Angeles, CA; American Chemical Society: Washington, DC, 1988; INOR 139, to be submitted for publication.